Retrodirective Distributed Transmit Beamforming with Two-Way Source Synchronization

Robert D. Preuss and D. Richard Brown III

***Abstract*—Distributed transmit beamforming has recently been proposed as a technique in which several single-antenna sources cooperate to form a virtual antenna array and simultaneously transmit with phase-aligned carriers such that the passband signals coherently combine at an intended destination. The power gains of distributed transmit beamforming can provide increased range, rate, energy efficiency, and/or security, as well as reduce interference. Distributed transmit beamforming, however, typically requires precise synchronization between the sources with timing errors on the order of picoseconds. In this paper, a new two-way synchronization protocol is developed to facilitate precise source synchronization and retrodirective distributed transmit beamforming. The two-way synchronization protocol is developed under the assumption that all processing at each source node is performed with local observations in local time. An analysis of the statistical properties of the phase and frequency estimation errors in the two-way synchronization protocol and the resulting power gain of a distributed transmit beamformer using this protocol is provided. Numerical examples are also presented characterizing the performance of distributed transmit beamforming in a system using two-way source synchronization. The numerical results demonstrate that near-ideal beamforming performance can be achieved with low synchronization overhead.**

I. Introduction

Distributed transmit beamforming is a technique in which multiple individual single-antenna sources simultaneously transmit a common message and control the phase and frequency of their carriers so that their bandpass signals constructively combine at an intended destination. The transmitters in a distributed transmit beamformer form a *virtual antenna array* and, in principle, can achieve all of the gains of a conventional antenna array, e.g. increased range, rate, and/or energy efficiency, without the size, cost, and complexity of a conventional antenna array. Distributed transmit beamforming can also provide benefits in terms of security and interference reduction since less transmit power is scattered in unintended directions.

A common assumption in the literature is that distributed transmit beamforming can be performed by using time-division-duplexing (TDD) and a phase conjugation technique similar to the retrodirective "Pon array" [1] technique developed for conventional antenna arrays. The approach is as follows: (i) the destination node first broadcasts a signal received by each source node and (ii) each source node then transmits back to the destination at the same frequency but with conjugate phase. In principle, the phase conjugation at each transmitter cancels the phase shift of the channel. This causes the carriers to arrive in phase and coherently combine at the destination.

While this retrodirective transmission technique is known to be effective for conventional antenna arrays where each antenna element is connected to a common local oscillator, it is actually likely to be ineffective in distributed transmission systems in which each source node has its own independent local oscillator *if the source nodes are not pre-synchronized*. To demonstrate the critical role of synchronization in distributed transmit beamforming, consider a system with two unsynchronized source nodes, denoted as S_1 and S_2, and one destination node. Denote the time at the destination node as t and the time at the source nodes as t_1 and t_2. For purposes of illustration, we assume that S_i has an unknown fixed local time offset with respect to the destination node's time such that $t_i = t + \Delta_i$.

Figure 1 shows a TDD timeline in which the unknown local clock offsets Δ_1 and Δ_2 are different, i.e. the source nodes are not pre-synchronized. In the first step of TDD operation, the destination node broadcasts the signal $x_0(t) = \exp\{j\omega_0 t\}\mathbb{I}_{t\in[0,T)}$ to the source nodes, where T is the signal duration and the indicator function $\mathbb{I}_{t\in\mathcal{A}} = 1$ when $t \in \mathcal{A}$, and is otherwise equal to zero. This signal is represented as the solid-line signal in Figure 1. Assuming single-path unit-gain channels and ignoring noise, the signal received by S_i can then be written as

$$y_i(t) = \exp\{j\omega_0(t-\tau_{0,i})\}\mathbb{I}_{t\in[\tau_{0,i},\tau_{0,i}+T)} \qquad (1)$$

for $i = 1, 2$ where $\tau_{0,i}$ is the unknown propagation delay of the channel from the destination node to S_i. These signals are illustrated as the solid-line signals on the source node's timelines in Figure 1. Note that (1) is written in the *destination node's* local time. In the *source node's* local time,

$$y_i(t_i) = \exp\{j\omega_0(t_i-\Delta_i-\tau_{0,i})\}\mathbb{I}_{t_i\in[\Delta_i+\tau_{0,i},\Delta_i+\tau_{0,i}+T)}$$

for $i = 1, 2$. The phase estimate at S_i is then calculated as the phase at $t_i = 0$, i.e. $-\omega_0(\Delta_i + \tau_{0,i})$.

In the second step of TDD operation, both source nodes transmit with conjugate phase back to the destination. The carrier transmitted by S_i can be written as

$$x_i(t_i) = \exp\{j\omega_0(t_i+\Delta_i+\tau_{0,i})\}\mathbb{I}_{t_i\in[s_i,s_i+T')} \qquad (2)$$

where T' is the transmission duration and s_i is the starting time of the transmission for source node i. These signals

R.D. Preuss is a Senior Member of the IEEE living in Arlington, MA 02476 USA. e-mail: r.preuss@ieee.org

D.R. Brown III is an Associate Professor with the Electrical and Computer Engineering Department, Worcester Polytechnic Institute, Worcester, MA 01609 USA. e-mail: drb@ece.wpi.edu.

This work was supported by NSF award CCF-0447743.

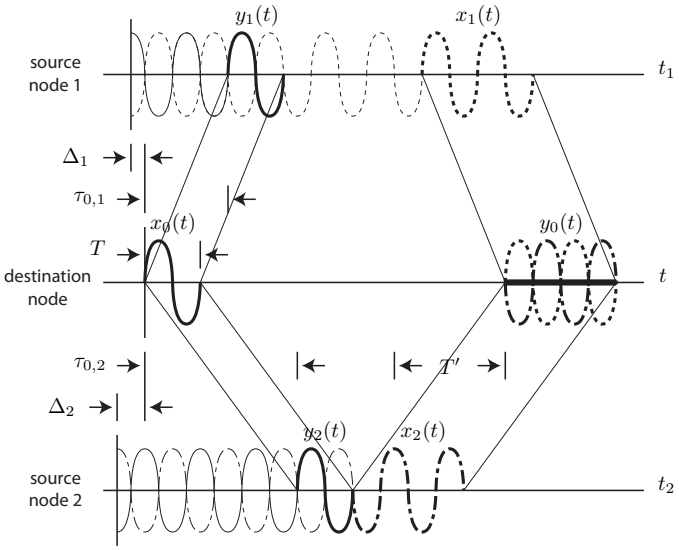

Fig. 1. An example of time-division-duplexing (TDD) in a system with two unsynchronized source nodes. The carriers transmitted by the source nodes in this example fully cancel each other at the destination node.

are shown as the dotted and dash-dotted signals for S_1 and S_2, respectively, on the source node's timelines in Figure 1. Converting (2) to the destination node's local time, we have

$$x_i(t) = \exp\{j\omega_0(t + 2\Delta_i + \tau_{0,i})\}\mathbb{I}_{t\in[s_i-\Delta_i, s_i-\Delta_i+T')}.$$

The aggregate signal received by the destination node after propagation from each source to the destination is then

$$y_0(t) = \sum_{i=1}^{2} \exp\{j\omega_0(t + 2\Delta_i)\}\mathbb{I}_{t\in[s_i', s_i'+T')} \tag{3}$$

where $s_i' := s_i - \Delta_i + \tau_{0,i}$. This last expression exposes the two elements of synchronization necessary to ensure coherent combining of the signals at the destination node. First, in order for the carriers to constructively combine, (3) requires that $2\omega_0\Delta_1 \equiv 2\omega_0\Delta_2 \pmod{2\pi}$. This condition is necessary and sufficient to achieve *carrier coherence*.

The second synchronization element required to ensure the signals coherently combine at the destination node relates to the start time of transmission at each source node. In order for source nodes' signals to arrive at the same time at the destination, the transmission start times must be staggered such that $s_1' = s_2'$. This condition is necessary and sufficient to achieve *message coherence*.

The focus of this paper is primarily on the problem of achieving carrier coherence since, as shown in this example, the effects of carrier offset can be critical. Moreover, carrier coherence is usually considered the more difficult problem because the synchronization accuracy required for carrier coherence is typically on the order of picoseconds. The problem of message coherence is also important and has been considered in [2], but the timing accuracy requirements are less stringent and the effects of message offset, i.e. intersymbol interference, are usually less critical.

Several carrier synchronization techniques have recently been proposed for distributed transmit beamforming including full-feedback closed-loop [3], one-bit closed-loop [4]–[6], master-slave open-loop [7], and round-trip open-loop carrier synchronization [8], [9]. Each of these techniques has advantages and disadvantages in particular applications, as discussed in the survey article [10].

In this paper, we describe a new synchronization technique called *two-way* synchronization [11] and demonstrate its efficacy in noise-free and noisy channels. Two-way synchronization is similar in some aspects to round-trip synchronization, but, unlike the round-trip carrier synchronization techniques described in [8], [9], two-way synchronization is performed among the source nodes prior to the transmission of a beacon from the intended destination.

The main contributions of this paper are a description of the two-way carrier synchronization technique in a system where each source node has an independent local oscillator. We also show how appropriate transmission phases can be generated to enable beamforming to an intended destination. We then analyze the statistical properties of the two-way synchronization protocol in terms of the estimation errors and oscillator phase noise. We conclude with numerical examples that show that the two-way synchronization overhead can be small with respect to the expected useful beamforming time.

II. System Model

We consider the system illustrated in Figure 2 one destination node, denoted as node 0, and M source nodes, denoted as nodes $\mathsf{S}_1, \ldots, \mathsf{S}_M$. All nodes are assumed to possess a single isotropic antenna. The channel between the destination node and S_m is modeled as a causal linear time-invariant (LTI) system with impulse response $g_m(t)$. The channel between S_m and S_n is also modeled as a causal linear time-invariant (LTI) system with impulse response $h_{m,n}(t)$ The noise in each channel is additive, white, and Gaussian and the impulse response of each channel in the system is assumed to be reciprocal, i.e. $h_{m,n}(t) = h_{n,m}(t)$.

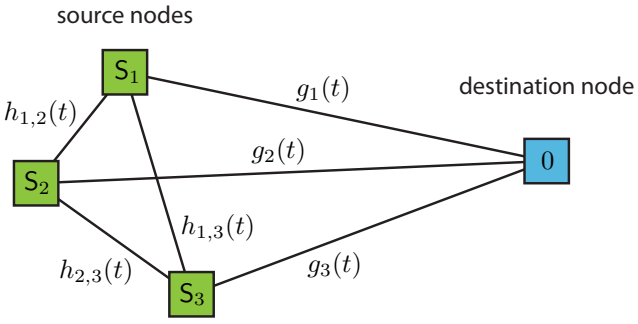

Fig. 2. A system with $M = 3$ source nodes and one destination node.

We assume the local time at S_i has an unknown rate offset β_i and an unknown time offset Δ_i with respect to a reference time t such that

$$t_i = \beta_i(t + \Delta_i). \tag{4}$$

This model does not include the effect of oscillator phase noise but is reasonable over short durations, e.g. during synchronization. The effects of oscillator phase noise during beamforming are considered in Section V.

III. Two-Way Source Synchronization Protocol

The two-way source synchronization protocol is initiated by S_1 transmitting a sinusoidal beacon to S_2. This sinusoidal beacon is retransmitted through increasing indices $\mathsf{S}_2 \rightarrow \mathsf{S}_3 \rightarrow \cdots \rightarrow \mathsf{S}_{M-1} \rightarrow \mathsf{S}_M$ ("forward propagation"), where each retransmission is a periodic extension of the beacon received in the previous timeslot. A second sinusoidal beacon, initiated by S_M, is similarly transmitted through the decreasing indices $\mathsf{S}_M \rightarrow \mathsf{S}_{M-1} \rightarrow \cdots \rightarrow \mathsf{S}_2 \rightarrow \mathsf{S}_1$ ("backward propagation"). Assuming approximately the same frequency is used for the forward and backward propagated beacons, $2M-2$ non-overlapping time slots (enumerated as $\mathsf{TS}^{(1)}, \ldots, \mathsf{TS}^{(2M-2)}$) are used to ensure there is no mutual interference among the $2M-2$ individual transmissions in the two-way source synchronization protocol.

The signals exchanged and estimates generated in each timeslot are explicitly described for the forward propagation stage as follows. In $\mathsf{TS}^{(1)}$, S_1 transmits a sinusoidal beacon $x_1^{(1)}(t_1) = \exp\{j(\omega_1 t_1 + \phi_1)\}\mathbb{I}_{t_1 \in T_1^{(1)}}$ to S_2 where $T_1^{(1)}$ is the transmission interval of S_1 in $\mathsf{TS}^{(1)}$. Note that $x^{(1)}(t_1)$ is expressed in local time for S_1. This beacon propagates through the channel to S_2 and is received in local time at S_2 as

$$y_2^{(1)}(t_2) = a_{1,2} \exp\left\{j\left(f_{1,2}(t_2) + \phi_1\right)\right\} \mathbb{I}_{t_2 \in T_2^{(1)}} + w_2^{(1)}(t_2)$$

where $T_2^{(1)}$ is the reception interval of S_2 in $\mathsf{TS}^{(1)}$, $w_2^{(1)}(t_2)$ is the noise in the signal received by S_2 in $\mathsf{TS}^{(1)}$, $f_{1,2}(t_2) := \beta_1\omega_1\left(\frac{t_2}{\beta_2} + \Delta_1 - \Delta_2\right) + \psi_{1,2}$, and $a_{1,2} = |H_{1,2}(\beta_1\omega_1)|$ and $\psi_{1,2} = \angle H_{1,2}(\beta_1\omega_1)$ are the amplitude and phase shift, respectively, of the LTI channel between S_1 and S_2 at the "true" frequency $\beta_1\omega_1$. This observation is then used by S_2 to generate frequency and phase estimates

$$\hat{\omega}_2^{(1)} = \frac{\beta_1\omega_1 + \tilde{\omega}_2^{(1)}}{\beta_2}, \text{ and} \tag{5}$$

$$\hat{\phi}_2^{(1)} = \beta_1\omega_1(\Delta_1 - \Delta_2) + \psi_{1,2} + \phi_1 + \tilde{\phi}_2^{(1)} \tag{6}$$

where $\tilde{\omega}_2^{(1)}$ and $\tilde{\phi}_2^{(1)}$ are the frequency and phase estimation error, respectively, at S_2 in $\mathsf{TS}^{(1)}$.

This process is repeated through increasing source node indices. In each timeslot, a source node transmits a periodic extension of the beacon it received in the prior timeslot to the next source node. The signal transmitted by S_{i-1} to S_i in $\mathsf{TS}^{(i-1)}$ is $x_{i-1}^{(i-1)}(t_{i-1}) = \exp\{j(\hat{\omega}_{i-1}^{(i-2)}t_{i-1} + \hat{\phi}_{i-1}^{(i-2)})\}\mathbb{I}_{t_{i-1} \in T_{i-1}^{(i-1)}}$. After propagation through the LTI channel to S_i, the signal is received as

$$y_i^{(i-1)}(t_i) = a_{i-1,i} \exp\left\{j\left(f_{i-1,i}(t_i) + \hat{\phi}_{i-1}^{(i-2)}\right)\right\} \mathbb{I}_{t_i \in T_i^{(i-1)}} + w_i^{(i-1)}(t_i)$$

where $f_{i-1,i} := \beta_{i-1}\hat{\omega}_{i-1}^{(i-2)}\left(\frac{t_i}{\beta_i} + \Delta_{i-1} - \Delta_i\right) + \psi_{i-1,i}$. This observation is then used by S_i to generate frequency and phase estimates

$$\hat{\omega}_i^{(i-1)} = \frac{\beta_{i-1}\hat{\omega}_{i-1}^{(i-2)} + \tilde{\omega}_i^{(i-1)}}{\beta_i}, \text{ and} \tag{7}$$

$$\hat{\phi}_i^{(i-1)} = \beta_{i-1}\hat{\omega}_{i-1}^{(i-2)}(\Delta_{i-1} - \Delta_i) + \psi_{i-1,i} + \hat{\phi}_{i-1}^{(i-2)} + \tilde{\phi}_i^{(i-1)} \tag{8}$$

for $i = 3, \ldots, M$, where $\tilde{\omega}_i^{(i-1)}$ and $\tilde{\phi}_i^{(i-1)}$ are the frequency and phase estimation error, respectively, at S_i in $\mathsf{TS}^{(i-1)}$. The forward propagation stage concludes at the end of $\mathsf{TS}^{(M-1)}$.

Backward propagation is the same as forward propagation except S_M initiates the process by transmitting a sinusoidal beacon $x_M^{(M)}(t_M) = \exp\{j(\omega_M t_M + \phi_M)\}\mathbb{I}_{t_M \in T_M^{(M)}}$ to S_{M-1}. The beacons are retransmitted through decreasing indices $i = M-1, \ldots, 1$ and the backward propagation stage concludes after S_1 receives the final beacon in $\mathsf{TS}^{(2M-2)}$.

At the end of the two-way source synchronization protocol, each source except S_1 and S_M has two sets of phase and frequency estimates. Sources S_1 and S_M use their initial beacon phase and frequency (ω_1 and ϕ_1 or ω_M and ϕ_M) as their other estimates. Note that these "estimates" have no estimation error. For notational convenience, we denote the four estimates obtained by S_i as $\hat{\omega}_{i,1}$, $\hat{\omega}_{i,2}$, $\hat{\phi}_{i,1}$, and $\hat{\phi}_{i,2}$.

IV. Synchronization and Beamforming

After the exchange of beacons, each source adds its first and second estimates to synthesize a synchronized local oscillator (SLO) with frequency $\hat{\omega}_i = \hat{\omega}_{i,1} + \hat{\omega}_{i,2}$ and initial phase $\hat{\phi}_i = \hat{\phi}_{i,1} + \hat{\phi}_{i,2}$. If we temporarily assume that each source node's phase and frequency estimates are perfect[1] in the sense that there is no estimation error in each timeslot, it is not difficult to show that the SLO phase $\xi_i := \hat{\omega}_i t_i + \hat{\phi}_i$ is identical at all source nodes (modulo 2π). To see this, we can use (7) in the forward propagation stage to write the first frequency estimate at S_i as

$$\hat{\omega}_{i,1} = \frac{\beta_{i-1}}{\beta_i}\hat{\omega}_{i-1,1} = \frac{\beta_1}{\beta_i}\omega_1$$

for $i = 2, \ldots, M$. The second equality results from a recursive application of the first equality and the fact that $\hat{\omega}_{1,1} := \omega_1$. Along the same lines, we can use (7) in the backward propagation stage to write the second frequency estimate at S_i as

$$\hat{\omega}_{i,2} = \frac{\beta_{i+1}}{\beta_i}\hat{\omega}_{i+1,2} = \frac{\beta_M}{\beta_i}\omega_M$$

for $i = M-1, \ldots, 1$ where $\hat{\omega}_{M,2} := \omega_M$. The resulting frequency at S_i is then

$$\hat{\omega}_i = \hat{\omega}_{i,1} + \hat{\omega}_{i,2} = \frac{\beta_1\omega_1 + \beta_M\omega_M}{\beta_i}. \tag{9}$$

The first phase estimate at S_i can be calculated from (7) and (8) in the forward propagation stage as

$$\begin{aligned}\hat{\phi}_{i,1} &= \beta_1\omega_1(\Delta_{i-1} - \Delta_i) + \psi_{i-1,i} + \hat{\phi}_{i-1,1} \\ &= \beta_1\omega_1(\Delta_1 - \Delta_i) + \sum_{\ell=1}^{i-1}\psi_{\ell,\ell+1} + \phi_1\end{aligned}$$

[1] Imperfect estimates are considered in Section V.

for $i = 2, \ldots, M$ where we have used $\beta_{i-1}\hat{\omega}_{i-1}^{(i-2)} = \beta_{i-1}\hat{\omega}_{i-1,1} = \beta_1\omega_1$ and where the second equality results from a recursive application of the first equality. Along the same lines, we can use (7) and (8) in the backward propagation stage to write the second phase estimate at S_i as

$$\hat{\phi}_{i,2} = \beta_M\omega_M(\Delta_M - \Delta_i) + \sum_{\ell=i}^{M-1} \psi_{\ell+1,\ell} + \phi_M$$

for $i = M-1, \ldots, 1$. Since $\psi_{\ell+1,\ell} = \psi_{\ell,\ell+1}$, i.e. the channels have reciprocal phase shifts, the resulting phase at S_i can be written as

$$\hat{\phi}_i = \beta_1\omega_1(\Delta_1 - \Delta_i) + \beta_M\omega_M(\Delta_M - \Delta_i) + \bar{\psi} + \phi_1 + \phi_M \quad (10)$$

where we have defined $\bar{\psi} := \sum_{\ell=1}^{M-1} \psi_{\ell,\ell+1}$.

Putting it all together, the SLO phase at S_i is then

$$\begin{aligned}\xi_i &= \frac{\beta_1\omega_1 + \beta_M\omega_M}{\beta_i} t_i + \beta_1\omega_1(\Delta_1 - \Delta_i) + \phi_1 \\ &\quad + \beta_M\omega_M(\Delta_M - \Delta_i) + \phi_M + \bar{\psi} \\ &= (\beta_1\omega_1 + \beta_M\omega_M)t + \gamma_1 + \gamma_M + \bar{\psi}\end{aligned}$$

where the second equality results from (4) and $\gamma_m := \beta_m\omega_m\Delta_m + \phi_m$. Hence, even though each source node possesses its own local notion of time and operates only on its own local estimates, each source node is able to synthesize a synchronized local oscillator after two-way synchronization.

After the formation of the SLOs, retrodirective distributed transmit beamforming can be performed using TDD techniques such as those described in [1]. For notational simplicity, assume that the destination's notion of time is reference time so that $t_0 = t$. After receiving the transmission from the destination at frequency ω_0, each source, for example, estimates the frequency and phase of this transmission and subtract these estimates, denoted as $\hat{\omega}_i^{(0)}$ and $\hat{\phi}_i^{(0)}$, respectively, from the SLO frequency and phase to generate the beamforming carrier

$$x_i^{(\mathsf{bf})}(t_i) = \exp\left\{ j\left((\hat{\omega}_i - \hat{\omega}_i^{(0)})t_i + \hat{\phi}_i - \hat{\phi}_i^{(0)} \right) \right\}. \quad (11)$$

Assuming again that the estimates are perfect, the sum of these carriers after propagation to the destination can be written as

$$y_0^{(\mathsf{bf})}(t) = \sum_{i=1}^{M} a_{0,i} \exp\left\{ j\left(\bar{\omega}t + \bar{\gamma} + \bar{\psi} \right) \right\} \mathbb{I}_{t \in T_{i,0}^{(\mathsf{bf})}} + w_0^{(\mathsf{bf})}(t)$$

where $\bar{\omega} := \beta_1\omega_1 + \beta_M\omega_M - \omega_0$ and $\bar{\gamma} := \gamma_1 + \gamma_M - \gamma_0$. The received power of the aggregate unmodulated carriers at the destination node in this case is $|y_0^{(\mathsf{bf})}(t)|^2 = (\sum_i a_{0,i})^2$. This corresponds to the power of an "ideal" transmit beamformer, when each source node transmits with unit carrier amplitude.

V. Performance Analysis with Estimation Error

Estimation errors incurred during two-way synchronization and source-destination channel phase estimation as well as phase noise at each source node all lead to some loss of performance with respect to the ideal transmit beamformer. At time t, the power of the aggregate carriers from the M source nodes received at the destination can be expressed as

$$|y_0^{(\mathsf{bf})}(t)|^2 = \sum_{m=1}^{M} a_{0,m}^2 + \sum_{m=1}^{M} \sum_{n \neq m} a_{0,m}a_{0,n} \cos\left(\delta_{m,n}(t)\right) \quad (12)$$

where the non-ideal nature of the distributed beamformer is captured in the carrier offset terms between S_m and S_n

$$\begin{aligned}\delta_{m,n}(t) := &(\hat{\omega}_m - \hat{\omega}_m^{(0)})\beta_m(t + \Delta_m) \\ &-(\hat{\omega}_n - \hat{\omega}_n^{(0)})\beta_n(t + \Delta_n) \\ &+(\hat{\phi}_m - \hat{\phi}_m^{(0)} + \psi_{m,0}) \\ &-(\hat{\phi}_n - \hat{\phi}_n^{(0)} + \psi_{n,0}) \\ &+\chi_m(t) - \chi_n(t)\end{aligned} \quad (13)$$

where $\chi_m(t) - \chi_n(t)$ represents the difference in the phase noise processes of the SLOs between S_m and S_n. Note that (13) is composed of three components: carrier frequency offset, initial carrier phase offset at $t = 0$, and phase noise. We can rewrite (13) in these terms as

$$\delta_{m,n}(t) = \tilde{\omega}_{m,n}t + \tilde{\phi}_{m,n} + \chi_{m,n}(t). \quad (14)$$

The frequency and phase estimates in (13) can be written as

$$\hat{\omega}_m = \frac{\beta_1\omega_1 + \beta_M\omega_M + \tilde{\omega}_m}{\beta_m}, \quad (15)$$

$$\hat{\omega}_m^{(0)} = \frac{\omega_0 + \tilde{\omega}_m^{(0)}}{\beta_m}, \quad (16)$$

$$\begin{aligned}\hat{\phi}_m = &\beta_1\omega_1(\Delta_1 - \Delta_m) + \beta_M\omega_M(\Delta_M - \Delta_m) \\ &+ \phi_1 + \phi_M + \bar{\psi} + \tilde{\phi}_m\end{aligned} \quad (17)$$

$$\hat{\phi}_m^{(0)} = \omega_0(\Delta_0 - \Delta_m) + \psi_{0,m} + \phi_0 + \tilde{\phi}_m^{(0)}. \quad (18)$$

Substituting these expressions into (13) allows us to write the frequency and phase offsets in (14) in terms of the individual estimation errors as

$$\tilde{\omega}_{m,n} = (\tilde{\omega}_m - \tilde{\omega}_m^{(0)}) - (\tilde{\omega}_n - \tilde{\omega}_n^{(0)}) \quad (19)$$

$$\begin{aligned}\tilde{\phi}_{m,n} = &(\tilde{\phi}_m - \tilde{\phi}_m^{(0)}) - (\tilde{\phi}_n - \tilde{\phi}_n^{(0)}) \\ &+ \Delta_m(\tilde{\omega}_m - \tilde{\omega}_m^{(0)}) - \Delta_n(\tilde{\omega}_n - \tilde{\omega}_n^{(0)}).\end{aligned} \quad (20)$$

The carrier frequency and phase offsets between S_m and S_n are analyzed in terms of the constituent estimation errors in the following sections. The statistical properties of the phase noise processes are discussed in Section V-D.

A. Frequency and Phase Estimation Error Statistics

To facilitate analysis, we assume all of the estimates are unbiased and that the estimation errors are jointly Gaussian distributed. It can be shown that the covariances $\mathrm{E}\{\hat{\omega}_m\hat{\omega}_n\}$, $\mathrm{E}\{\hat{\phi}_m\hat{\phi}_n\}$, $\mathrm{E}\{\hat{\omega}_m^{(0)}\hat{\omega}_n^{(0)}\}$, and $\mathrm{E}\{\hat{\phi}_m^{(0)}\hat{\phi}_n^{(0)}\}$ are all zero except when $m = n$ since observations in different timeslots are affected by independent noise realizations and observations at different source nodes are also affected by independent noise realizations. It can also be shown that all of the other covariances are zero except $\mathrm{E}\{\hat{\omega}_m\hat{\phi}_m\}$ and $\mathrm{E}\{\hat{\omega}_m^{(0)}\hat{\phi}_m^{(0)}\}$ since frequency and phase estimates obtained from the same observation at a particular source node are not independent.

It is possible to bound the non-zero covariances with the Cramer-Rao bound (CRB) [12]. Given an N_s-sample observation of a complex exponential of amplitude a, the CRB for the covariance of the frequency and phase estimates is [13]

$$\mathrm{cov}\left\{[\omega,\phi]^\top\right\} \geq \frac{\sigma^2}{a^2}\begin{bmatrix} \frac{1}{T_s^2 N_s(Q-P^2)} & \frac{-(n_0+P)}{T_s N_s(Q-P^2)} \\ \frac{-(n_0+P)}{T_s N_s(Q-P^2)} & \frac{n_0^2+2n_0P+Q}{N_s(Q-P^2)} \end{bmatrix} \quad (21)$$

where σ^2 is the variance of the uncorrelated real and imaginary components of the independent, identically distributed, zero-mean, complex Gaussian noise samples, T_s is the sampling period, n_0 is the index of the first sample of the observation in the observer's local time, $P := (N_s-1)/2$, $Q := (N_s-1)(2N_s-1)/6$, and $\boldsymbol{A} \geq \boldsymbol{B}$ means that $\boldsymbol{A}-\boldsymbol{B}$ is positive semidefinite. These results can be used as a reasonable approximation for the non-zero covariances when each source node uses an unbiased and efficient estimator, e.g. the maximum likelihood estimator for large N_s [12], to generate the local phase and frequency estimates.

B. Carrier Frequency Offset

In the forward propagation stage of the two-way synchronization protocol, the estimation error $\tilde{\omega}_i^{(i-1)}$ in (7) is defined with respect to the "true" frequency of the signal transmitted by S_{i-1} in $\mathsf{TS}^{(i-1)}$. In $\mathsf{TS}^{(1)}$, the true frequency of transmission is $\beta_1\omega_1$. In $\mathsf{TS}^{(i-1)}$ for $i=3,\ldots,M$, the true frequency of transmission is $\beta_{i-1}\hat{\omega}_{i-1}^{(i-2)}$. The serial nature of the transmissions in the two-way synchronization protocol implies that the frequency error at S_i with respect to the initial true beacon frequency $\beta_1\omega_1$ is an accumulation of the individual frequency estimation errors, i.e. $\tilde{\omega}_2^{(1)}+\cdots+\tilde{\omega}_i^{(i-1)}$. The same is true for the backward propagation stage except the true frequency of the initial beacon is $\beta_M\omega_M$.

The frequency error of the SLO at S_m can thus be computed from recursive application of (7) for the forward and backward propagation stages as

$$\tilde{\omega}_m \;=\; \sum_{\ell=2}^{m}\tilde{\omega}_\ell^{(\ell-1)} + \sum_{\ell=m}^{M-1}\tilde{\omega}_\ell^{(2M-\ell-1)} \quad (22)$$

where the first and second sums correspond to the accumulated estimation error at S_i in the forward and backward propagation stages, respectively. Based on (19) and the assumptions in Section V-A, this result shows that the carrier frequency offsets between S_m and S_n are zero-mean and jointly Gaussian distributed with covariances that can be straightforwardly computed in terms of the constituent estimation error covariances.

C. Carrier Phase Offset

Similar to the frequency estimation errors, the phase estimation errors in the forward and backward propagation stages of the two-way synchronization protocol accumulate as the signals propagate through increasing and decreasing source node indices. The accumulation of phase error at S_i, however, is due to both constituent phase and frequency estimation errors. In the forward propagation stage of the two-way synchronization protocol, we can recursively apply (7) and (8) to write the first local phase estimate at S_m as

$$\hat{\phi}_m^{(i-1)} = \beta_1\omega_1(\Delta_1-\Delta_m)+\phi_1+\sum_{\ell=2}^{m}\psi_{\ell-1,\ell} + \sum_{\ell=2}^{m}\tilde{\phi}_\ell^{(\ell-1)} + \sum_{\ell=2}^{m-1}\tilde{\omega}_\ell^{(\ell-1)}(\Delta_\ell-\Delta_m)$$

for $m=2,\ldots,M$. Similarly, the second local phase estimate obtained during backward propagation at S_m is

$$\hat{\phi}_m^{(2M-m-1)} = \beta_M\omega_M(\Delta_M-\Delta_m)+\phi_M+\sum_{\ell=m}^{M-1}\psi_{\ell,\ell+1} + \sum_{\ell=m}^{M-1}\tilde{\phi}_\ell^{(2M-\ell-1)} + \sum_{\ell=m+1}^{M-1}\tilde{\omega}_\ell^{(2M-\ell-1)}(\Delta_\ell-\Delta_m)$$

for $m=1,\ldots,M-1$. These estimates are summed at S_m to generate the SLO phase. The resulting phase error is then

$$\tilde{\phi}_i = \sum_{\ell=2}^{i}\tilde{\phi}_\ell^{(\ell-1)} + \sum_{\ell=2}^{i-1}\tilde{\omega}_\ell^{(\ell-1)}(\Delta_\ell-\Delta_i) + \sum_{\ell=i}^{M-1}\tilde{\phi}_\ell^{(2M-\ell-1)} + \sum_{\ell=i+1}^{M-1}\tilde{\omega}_\ell^{(2M-\ell-1)}(\Delta_\ell-\Delta_i).$$

Based on (20), (22), and the assumptions in Section V-A, this result shows that the carrier phase offsets between S_m and S_n are zero-mean and jointly Gaussian distributed with covariances that can be straightforwardly computed in terms of the constituent estimation error covariances.

D. Phase Noise

Phase noise causes the phase of the SLO at each source node to randomly wander from the phase obtained at the end of the two-way synchronization protocol. As shown in [9], this can establish a ceiling on the reliable beamforming time even in the absence of estimation error.

The phase noise $\chi_i(t)$ at S_i can be modeled as a zero-mean non-stationary Gaussian random process, independent of the estimation errors, with variance increasing linearly with time, i.e. $\sigma_{\chi_i}^2(t) = r(t-T_i^{(\mathsf{sync})})$ for $t \geq T_i^{(\mathsf{sync})}$, where $T_i^{(\mathsf{sync})}$ is the time at which S_i generates estimates $\hat{\omega}_i$ and $\hat{\phi}_i$. The variance parameter r is a function of the physical properties of the oscillator including its natural frequency and physical type [14]. We assume that all source nodes share the same value of r but have independent phase noise processes.

VI. Numerical Results

This section presents numerical examples of the performance retrodirective distributed transmit beamforming in a system using two-way source synchronization. To provide a fair comparison with single-source transmission, we normalize the transmit power of each source node by M so that the total transmit power is fixed. We compute the mean beamforming gain with respect to single-source transmission.

The scenario considered in this section assumes 1 ms observations during the forward and backward propagation

stages of the two-way synchronization protocol. All channels are assumed to have unit gain and all signals are assumed to be received at a signal to noise ratio of 10dB. At the conclusion of the final synchronization timeslot, the source nodes form their SLOs and the destination immediately broadcasts a 1 ms beacon. The CRB results in (21) are used to generate the jointly Gaussian constituent estimation errors with appropriate covariances. The beamforming power at the destination for each realization of the estimation errors and phase noise processes is computed using the results in Section V.

Figure 3 shows the beamforming gain as a function of time for different numbers of source nodes (M) and different levels of local oscillator phase noise (r). The $r = 0$ results correspond to the case with no phase noise and isolate the effect of carrier phase and frequency offsets on the mean beamforming gain. The $r = 1$ results correspond to the case when the each source node has an independent phase noise process typical of a low-cost oscillator. In this case, as expected, the mean beamforming gain degrades more quickly. In both cases, periodic resynchronization is necessary to prevent the nodes from slipping out of synchronicity and transmitting incoherently. The overhead required for periodic resynchronization, however, can be low with respect to the amount of beamforming time. For example, in the case with $M = 8$ source nodes, the mean beamforming gain of source nodes with low-cost oscillators is within 1dB of ideal for approximately 240 ms. The synchronization time in this case is 14 ms, corresponding to an overhead of approximately 5%. Even lower overheads can be achieved by using oscillators with better phase noise characteristics, e.g. temperature controlled oscillators.

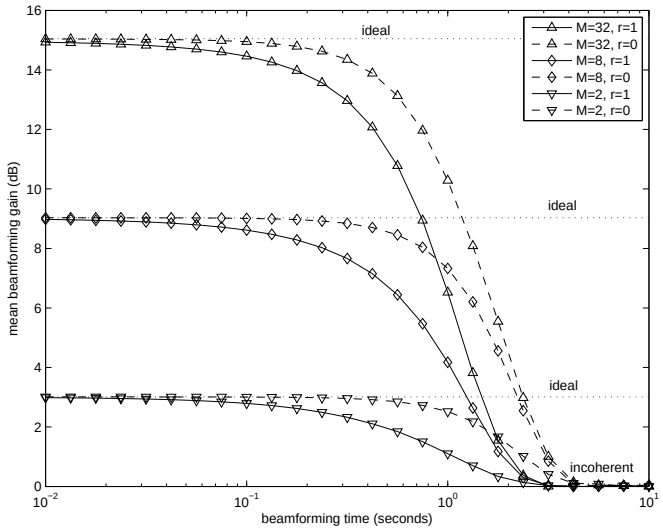

Fig. 3. Mean received beamforming gain as a function of beamforming time, number of source nodes, and local oscillator phase noise parameter.

The results in Figure 3 also show that increasing the number of source nodes participating in the distributed transmit beamformer increases the mean received power at the destination, up to the point in time when incoherent transmission begins. The performance gap with respect to ideal, however, tends to be larger when M is large because the amount of time spent synchronizing the nodes leads to larger initial phase offsets at the start of beamforming.

VII. Conclusion

This paper presented the two-way carrier synchronization protocol and described its use in retrodirective distributed transmit beamforming. An analysis of the statistical properties of the phase and frequency estimation errors and resulting power of a retrodirective distributed transmit beamformer was also provided. Numerical examples characterizing the performance of a distributed transmit beamformer in a system using two-way synchronization were presented and demonstrated that near-ideal beamforming performance can be achieved with low synchronization overhead.

References

[1] C. Pon, "Retrodirective array using the heterodyne technique," *IEEE Trans. on Antennas and Prop.*, vol. 12, no. 2, pp. 176–180, Mar 1964.

[2] V. Jungnickel, T. Wirth, M. Schellmann, T. Haustein, and W. Zirwas, "Synchronization of cooperative base stations," in *IEEE Int. Symp. on Wireless Communication Systems (ISWCS)*, October 2008, pp. 329–334.

[3] Y. Tu and G. Pottie, "Coherent cooperative transmission from multiple adjacent antennas to a distant stationary antenna through AWGN channels," in *IEEE Vehicular Technology Conf. (VTC)*, vol. 1, Birmingham, AL, Spring 2002, pp. 130–134.

[4] R. Mudumbai, J. Hespanha, U. Madhow, and G. Barriac, "Scalable feedback control for distributed beamforming in sensor networks," in *IEEE International Symp. on Information Theory (ISIT)*, Adelaide, Australia, September 2005, pp. 137–141.

[5] R. Mudumbai, B. Wild, U. Madhow, and K. Ramchandran, "Distributed beamforming using 1 bit feedback: from concept to realization," in *44th Allerton Conf. on Comm., Control, and Computing*, Monticello, IL, Sep. 2006, pp. 1020 – 1027.

[6] R. Mudumbai, J. Hespanha, U. Madhow, and G. Barriac, "Distributed transmit beamforming using feedback control," *IEEE Trans. on Information Theory*, in review.

[7] R. Mudumbai, G. Barriac, and U. Madhow, "On the feasibility of distributed beamforming in wireless networks," *IEEE Trans. on Wireless Communications*, vol. 6, no. 5, pp. 1754–1763, May 2007.

[8] D.R. Brown III, G. Prince, and J. McNeill, "A method for carrier frequency and phase synch. of two autonomous cooperative transmitters," in *IEEE Signal Proc. Advances in Wireless Comm. (SPAWC)*, New York, NY, June 5-8, 2005, pp. 278–282.

[9] D.R. Brown III and H.V. Poor, "Time-slotted round-trip carrier synchronization for distributed beamforming," *IEEE Trans. on Signal Processing*, vol. 56, no. 11, pp. 5630–5643, November 2008.

[10] R. Mudumbai, D.R. Brown III, U. Madhow, and H.V. Poor, "Distributed transmit beamforming: Challenges and recent progress," *IEEE Communications Magazine*, vol. 47, no. 2, pp. 102–110, February 2009.

[11] R. D. Preuss and T. P. Bidigare, "Methods and systems for distributed synchronization," U.S. Patent Application 12/383,192, March 19, 2009.

[12] H.V. Poor, *An Introduction to Signal Detection and Estimation*, 2nd ed. New York: Springer-Verlag, 1994.

[13] D. Rife and R. Boorstyn, "Single-tone parameter estimation from discrete-time observations," *IEEE Trans. on Information Theory*, vol. 20, no. 5, pp. 591–598, September 1974.

[14] A. Demir, A. Mehrotra, and J. Roychowdhury, "Phase noise in oscillators: A unifying theory and numerical methods and characterization," *IEEE Trans. on Circuits and Systems I: Fund. Theory and Appl.*, vol. 47, no. 5, pp. 655–674, May 2000.